

## Electronic Supplementary Information (ESI)

# Highly Connected Hierarchical Textured TiO<sub>2</sub> Spheres as Photoanodes for Dye-sensitized Solar Cells

Jianjian Lin,<sup>a,b</sup> Andrew Nattestad,<sup>\*c</sup> Hua Yu,<sup>b</sup> Yang Bai,<sup>b</sup> Lianzhou Wang,<sup>\*b</sup> Shi Xue Dou,<sup>a</sup> Jung Ho Kim,<sup>\*a</sup>

<sup>a</sup> Institute for Superconducting and Electronic Materials (ISEM), Australian Institute for Innovative Materials (AIIM), University of Wollongong, NSW 2522, Australia. E-mail: [jhk@uow.edu.au](mailto:jhk@uow.edu.au)

<sup>b</sup> Nanomaterials Centre, School of Chemical Engineering and Australian Institute for Bioengineering and Nanotechnology, The University of Queensland, Brisbane, QLD 4072, Australia. E-mail: [l.wang@uq.edu.au](mailto:l.wang@uq.edu.au)

<sup>c</sup> Intelligent Polymer Research Institute, ARC Centre of Excellence for Electromaterials Science, AIIM, University of Wollongong, NSW 2522, Australia. E-mail: [anattest@uow.edu.au](mailto:anattest@uow.edu.au)

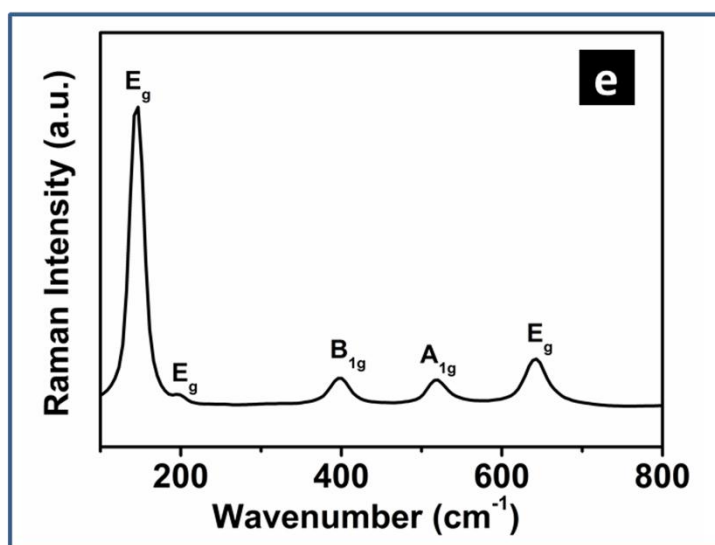
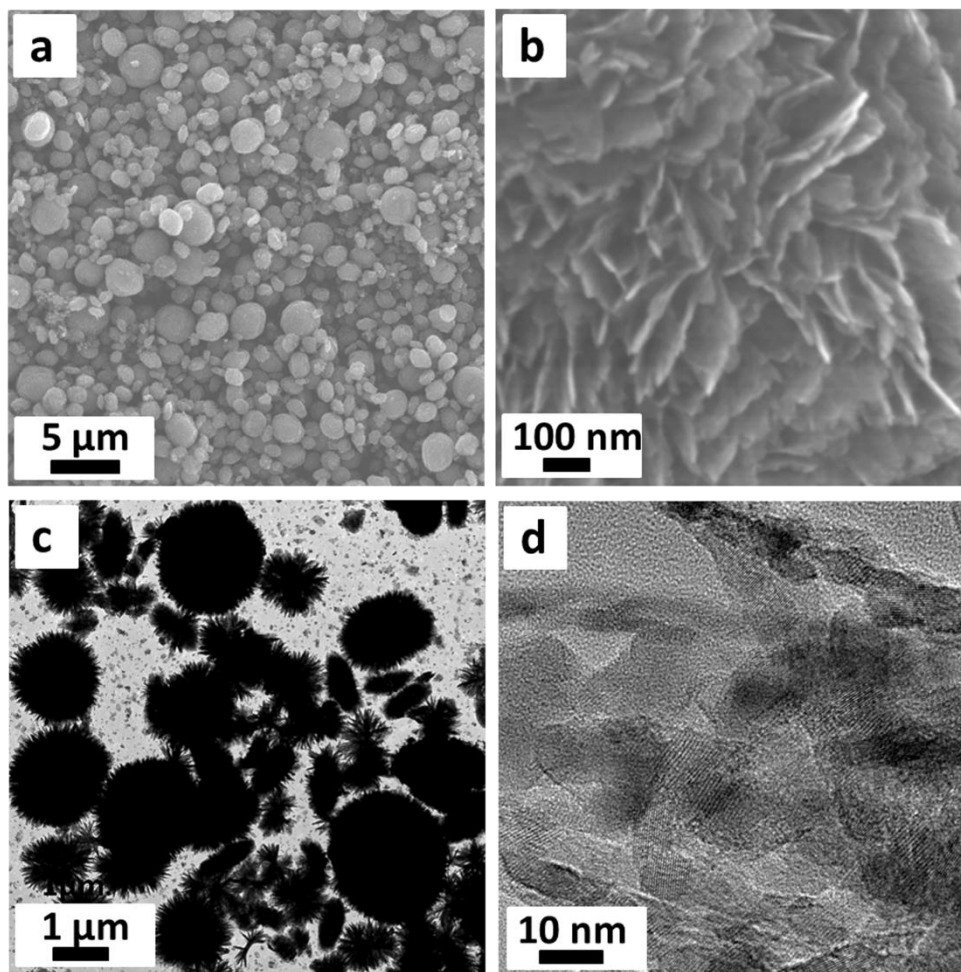


**Fig. S1** (a) Low magnification SEM image of the calcined HCHT, (b) higher magnification image of the nanosheet building blocks, (c) low magnification TEM image of the urchin-like spheres, (d) enlarged TEM image of the nanosheet building blocks; (e) Raman spectrum of the calcined HCHT clearly identifies the anatase phase from the characteristic Raman modes at  $142.1\text{ cm}^{-1}$  ( $E_g$ ),  $194.5\text{ cm}^{-1}$  ( $E_g$ ),  $396.1\text{ cm}^{-1}$  ( $B_{1g}$ ),  $515.8\text{ cm}^{-1}$  ( $A_{1g}$ ), and  $638.4\text{ cm}^{-1}$  ( $E_g$ ), which can be assigned to the Raman active modes ( $A_{1g}+B_{1g}+3E_g$ ) of anatase.

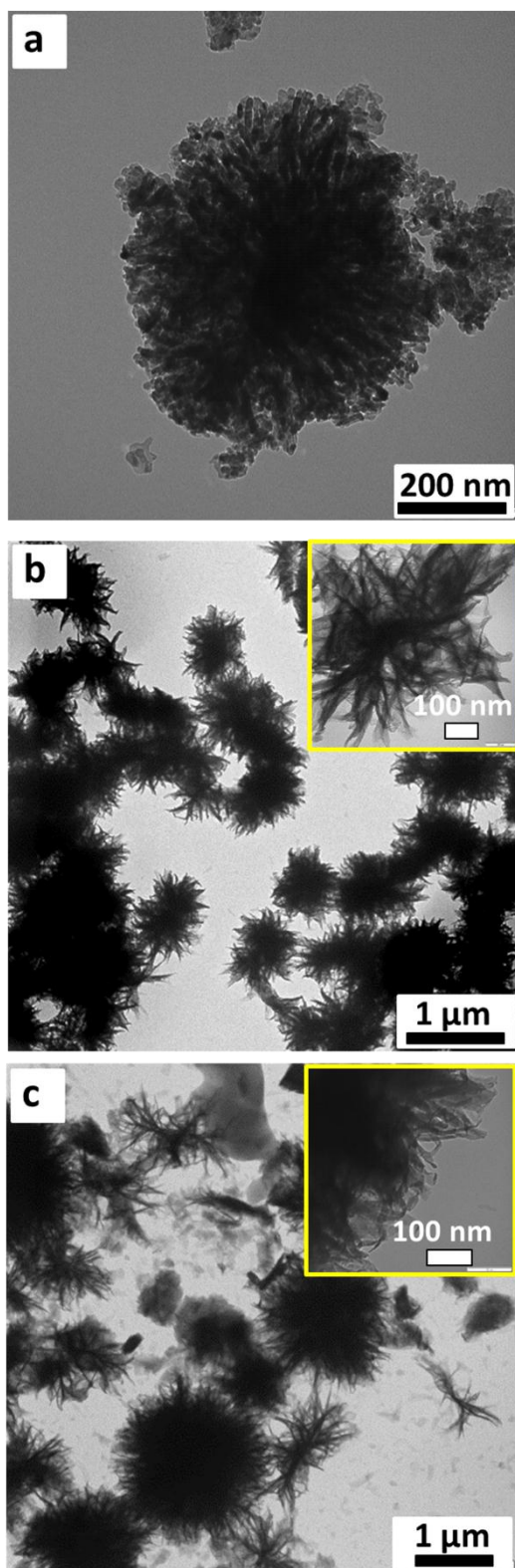


**Fig. S2** TEM images, with the insets showing higher magnification, of as-prepared precipitates obtained after different reaction times (a) 1 h, (b) 5 h, (c) 12 h, via hydrothermal reaction of a solution containing 0.5 mL TB and 30 mL HAc at 150 °C.

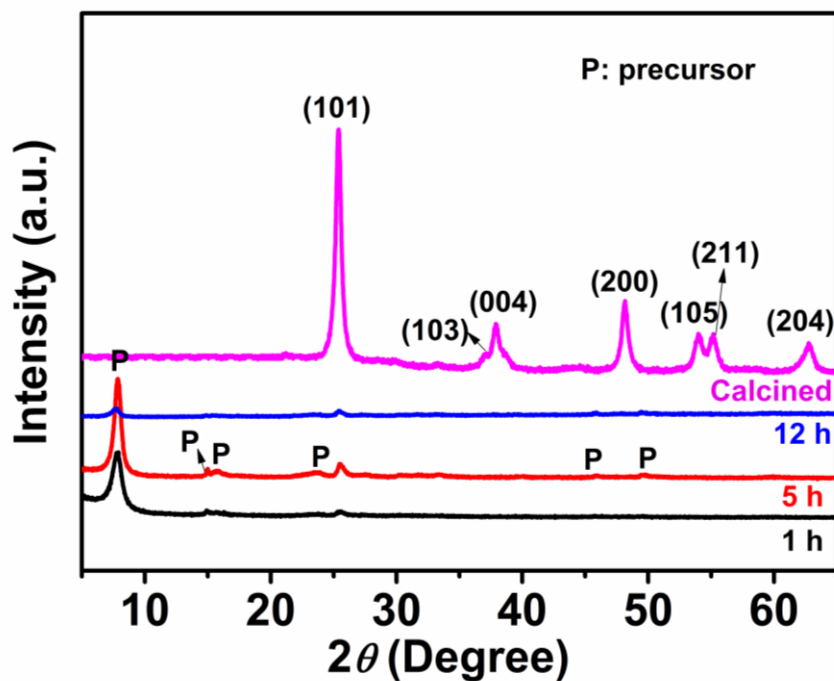


**Fig. S3** XRD patterns of as-prepared precipitates obtained after different reaction times via hydrothermal reaction of a solution containing 0.5 mL TB and 30 mL HAc at 150 °C, as well as a sample obtained after 12 h of reaction and 3 h of calcination at 500 °C.

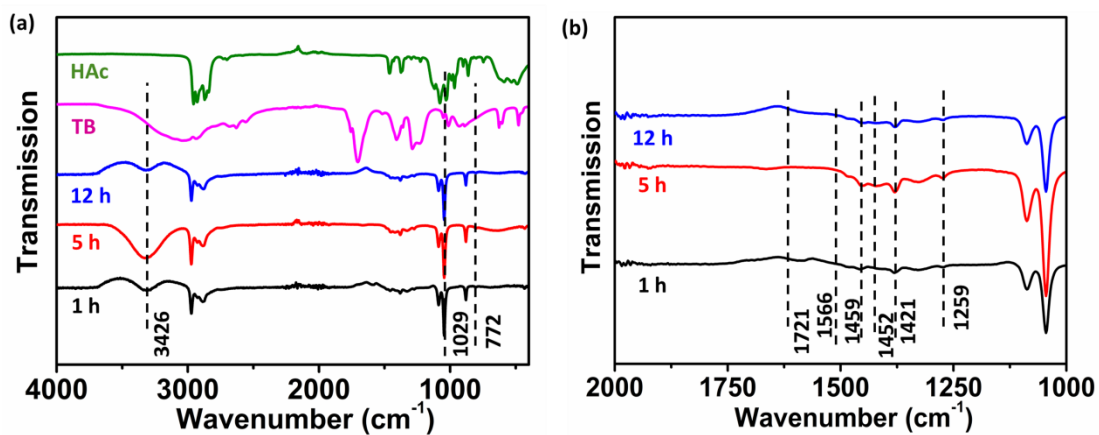


**Fig. S4** (a) FTIR spectra of HAc, TB, and the precipitates obtained after different reaction times via a hydrothermal reaction of a solution containing 0.5 mL TB and 30 mL HAc at 150 °C; (b) magnification of (a) in the range of 1000-2000  $\text{cm}^{-1}$ .

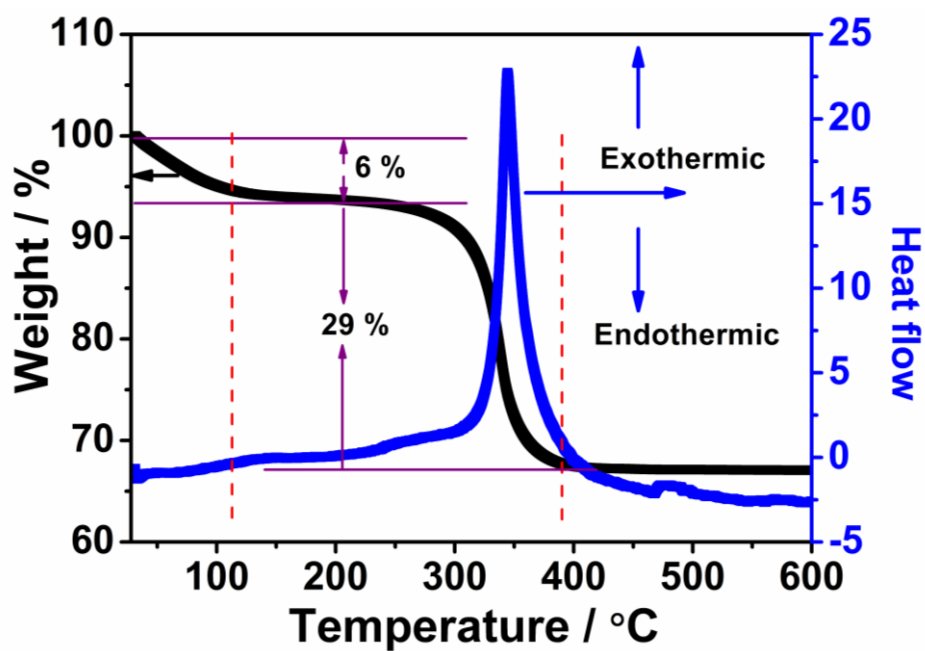


**Fig. S5** Thermogravimetric analysis and differential scanning calorimetry curves of the dried precipitate prepared via hydrothermal reaction of a solution containing 0.5 mL TB and 30 mL HAc at 150 °C for 12 h.

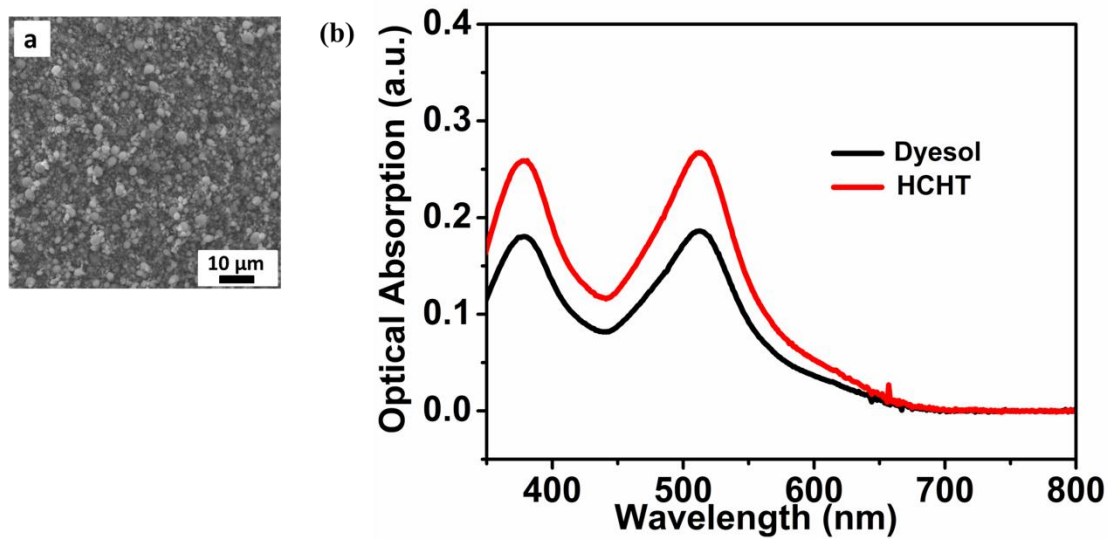


**Fig. S6** (a) Top-view SEM image of HCHT film on FTO glass. (b) Optical absorption of dye desorbed from the Dyesol and HCHT films by dissolving it in 0.1 M NaOH.

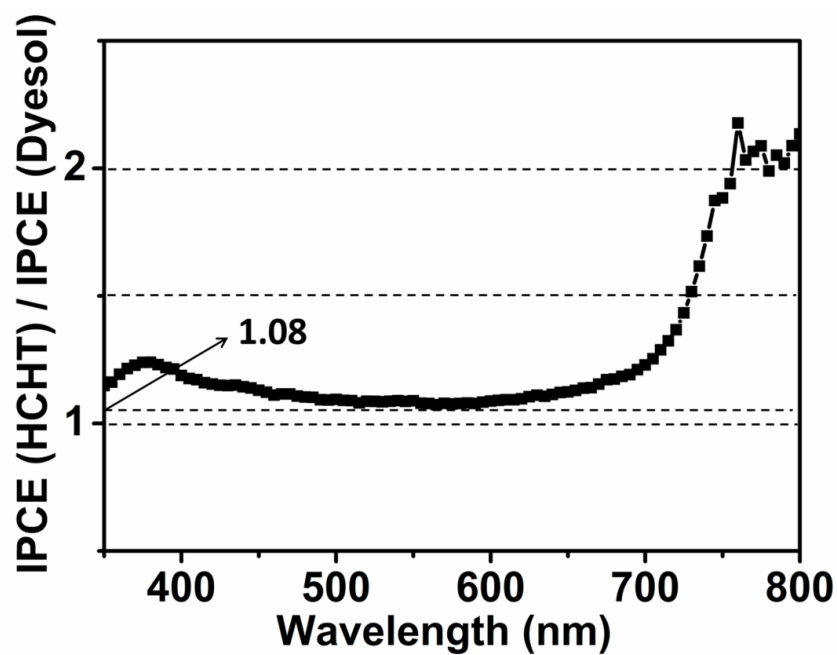


**Fig. S7** Ratio of IPCE value of HCHT to that of Dyesol, depending on the wavelength of the incident light.

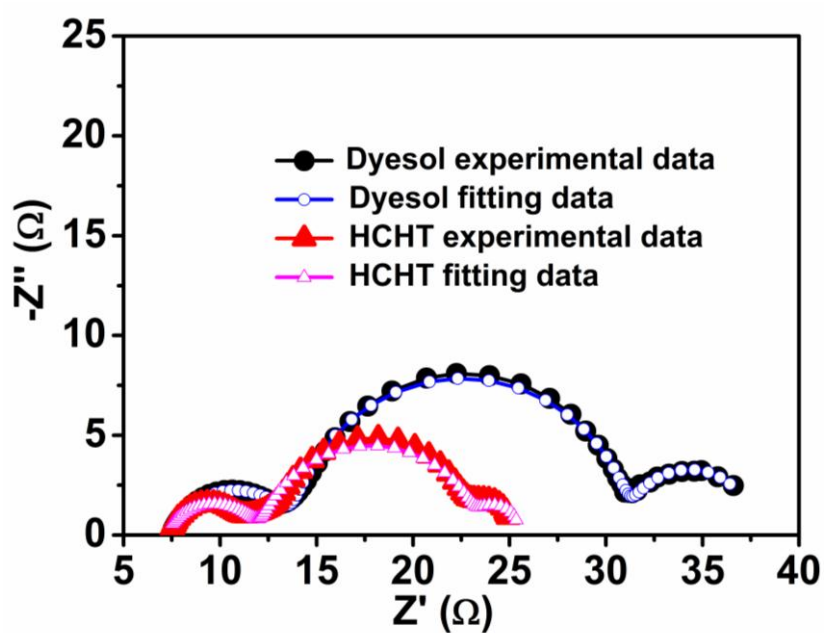


**Fig. S8** Impedance spectra of DSCs containing Dyesol and IHTT photoanodes measured at  $V_{oc}$  under illumination at  $100 \text{ mW cm}^{-2}$ : Nyquist plots, with the experimental data and the fitting data.

**Table S1** Series resistances of Dyesol- and HCHT-based DSCs.

Samples	$R_s$ ( $\Omega$ )	$R_{ct1}$ ( $\Omega$ )	$R_{ct2}$ ( $\Omega$ )	$R_{diff}$ ( $\Omega$ )
Dyesol	7.4	6.4	17.6	6.3
HCHT	7.2	4.9	11.5	1.9